






RECyT

Year 28 / N° 45 / 2026 /

DOI: <https://doi.org/10.36995/j.recyt.2026.45.009>

## Optimization and evaluation of encapsulated enzymatic formulations of *Trichoderma koningiopsis* strains for phytopathogen fungal biocontrol

### Optimización y evaluación de formulaciones enzimáticas encapsuladas de *Trichoderma koningiopsis* para biocontrol de hongos fitopatógenos

Marcela P., Barengo<sup>1,2,\*</sup> ; David K., Schmidt<sup>1</sup> ; Pedro D., Zapata<sup>1,2</sup> ; Gustavo A., Bich<sup>1,2</sup> ; María L., Castrillo<sup>1,2</sup> 

1- Laboratorio de Biotecnología Molecular. Instituto de Biotecnología Misiones “Dra. María Ebe Reca” (InBioMis). Facultad de Ciencias Exactas Químicas y Naturales. Universidad Nacional de Misiones. Ruta 12 Km 7 ½ (3300), Misiones, Argentina.

2- Consejo Nacional de Investigaciones Científicas y Técnicas (CONICET). Buenos Aires, Argentina.

\*E-mail: [barengomarcela@gmail.com](mailto:barengomarcela@gmail.com)

Received: 27/02/2026; Accepted: 15/04/2026

#### Abstract

Sustainable agriculture requires effective alternatives, and enzyme-based biocontrol strategies derived from *Trichoderma* represent a promising approach. However, field application of enzymatic supernatants is often limited by low stability and rapid loss of activity. This study aimed to optimize the encapsulation of enzymatic supernatants from native strains *Trichoderma koningiopsis* LBM 116 and LBM 219 using sodium alginate, and to evaluate the functional performance of the resulting formulations. A Box–Behnken response surface design identified optimal encapsulation conditions (1% alginate, 1% CaCl<sub>2</sub>, 0.5 mm cannula diameter), yielding spherical capsules (~1300 μm). Proteases exhibited high encapsulation efficiency (up to 84.8%) and strong operational stability, whereas β-1,3-glucanases showed moderate retention and progressive activity loss. Chitinase activity was not retained within the alginate matrix. Despite partial enzyme leakage, encapsulated formulations significantly inhibited the growth of *Fusarium oxysporum* LBM 232, maintaining antifungal efficacy comparable to free supernatants. These findings demonstrate that alginate-based encapsulation is a viable strategy for stabilizing mycolytic enzymes; however, matrix reinforcement will be necessary to achieve full retention of the enzymatic complex and enhance long-term performance in agricultural systems.

**Keywords:** Immobilization, Sodium alginate, Proteases, β-1,3-glucanases, *Fusarium*.

#### Resumen

La agricultura sostenible requiere alternativas eficaces y el biocontrol basado en enzimas derivadas de *Trichoderma* constituye un enfoque prometedor. Sin embargo, su aplicación se ve limitada por su baja estabilidad y la rápida pérdida de actividad. Este estudio tuvo como objetivo optimizar la encapsulación de sobrenadantes enzimáticos de las cepas nativas *Trichoderma koningiopsis* LBM 116 y LBM 219 mediante alginato de sodio y evaluar el desempeño funcional de las formulaciones obtenidas. Un diseño de superficie de respuesta Box-Behnken permitió identificar las condiciones óptimas de encapsulación (1 % de alginato, 1 % de CaCl<sub>2</sub>, aguja de 0,5 mm) y generar cápsulas esféricas (~1300 μm). Las proteasas mostraron alta eficiencia de encapsulación (hasta 84,8 %) y elevada estabilidad operativa, mientras que las β-1,3-glucanasas presentaron retención moderada y pérdida progresiva de actividad. Las quitinasas no se retuvieron en la matriz de alginato. A pesar de la fuga parcial de enzimas, las formulaciones encapsuladas inhibieron significativamente el crecimiento de *Fusarium oxysporum* LBM 232, con eficacia comparable a los sobrenadantes libres. Estos resultados demuestran que la encapsulación es una estrategia viable para estabilizar enzimas micólicas; no obstante, será necesario reforzar la matriz para lograr la retención completa del complejo enzimático y mejorar su desempeño a largo plazo en sistemas agrícolas.

**Palabras clave:** Inmovilización, Alginato de sodio, Proteasas, β-1,3-glucanasas, *Fusarium*.

#### INTRODUCTION

Modern agriculture has increased productivity through the intensive use of synthetic pesticides; however, this model has generated significant

environmental and health concerns, including soil and water contamination and adverse effects on non-target organisms (1–3). These limitations have intensified the search for sustainable

production strategies that reduce dependence on agrochemicals while preserving biodiversity, human health, and the environment. In this context, bio-inputs have emerged as viable alternatives in contemporary agricultural systems (4–6).

Among these, microbial antagonists are some of the most promising tools due to their diverse mechanisms of action, including the production of antifungal secondary metabolites, secretion of cell wall-degrading enzymes (CWDEs), and induction of plant defense responses (7–12). Species of the genus *Trichoderma* are particularly relevant, as they combine strong antagonistic activity against phytopathogens with plant growth-promoting capabilities and have been widely studied at both global and regional levels (13–16).

On the other hand, the use of native isolates is a strategic approach, given their adaptation to local edaphoclimatic conditions and their potential to reduce dependence on imported commercial strains (17–19).

Among phytopathogenic fungi, *Fusarium oxysporum* is one of the most relevant species, causing vascular wilt diseases affecting a wide range of crops, including *Ilex paraguariensis* (yerba mate), a perennial crop of high economic importance in northeastern Argentina (NEA) (20; 21). In this system, *Fusarium* spp. have been associated with root rot and decline processes that compromise plant establishment and long-term productivity.

These soilborne pathogens represent a major constraint, and their ability to persist in soil through resistant structures and survive as saprophytes enhances their epidemiological relevance, particularly in warm and humid environments such as those of the NEA region.

In this context, the enzymatic machinery of *Trichoderma*, particularly chitinases,  $\beta$ -1,3-glucanases, and proteases, plays a central role in mycoparasitism by directly degrading fungal cell walls (22–27). Enzymatic supernatants derived from these fungi therefore represent a valuable resource for the development of enzyme-based antifungal bioformulations. However, their field application is often limited by environmental instability, as fluctuations in pH, temperature, and humidity can reduce catalytic activity and persistence (28–30).

To address this limitation, enzyme immobilization via encapsulation techniques has emerged as an innovative and promising technological strategy. Encapsulation involves incorporating an active core—such as microorganisms, metabolites, or enzymes—into a protective matrix, typically composed of natural biopolymers, alginate and chitosan. This matrix acts as a physical barrier against adverse environmental conditions, prolongs the shelf life of the active ingredient

during storage, improves stability under variable environmental conditions, and enables controlled release at the desired site and time (31–34). In the specific case of enzymes, immobilization has been shown to increase structural stability, reduce loss of catalytic activity, and promote reuse in complex systems, including heterogeneous matrices such as soil (35; 36).

The encapsulation of fungal enzymatic supernatants represents an emerging field with high potential to transform unstable enzyme cocktails into next-generation bio-inputs capable of maintaining activity under varying environmental conditions for extended periods. Based on this background and considering the need to overcome the limitations associated with bio-input stability under field conditions, this study aimed to optimize the encapsulation technique for enzymatic supernatants produced by the native isolates *Trichoderma koningiopsis* LBM 116 and LBM 219, characterize the resulting capsules physicochemically and functionally, and evaluate their antifungal capacity against the phytopathogen *Fusarium oxysporum* LBM 232. This study seeks to advance the development of encapsulated enzymatic formulations with potential applications in sustainable agricultural systems.

## MATERIALS AND METHODS

### Microorganisms

Three native fungal strains from Misiones (Argentina) were used in this study: *Trichoderma koningiopsis* LBM 116, *T. koningiopsis* LBM 219, and *Fusarium oxysporum* LBM 232. All strains belong to the culture collection of the Molecular Biotechnology Laboratory at the Misiones Biotechnology Institute (InBioMis), National University of Misiones (UNaM), Argentina. In compliance with the Nagoya Protocol on Access and Benefit-sharing, authorization for all microorganisms collection was obtained from the Institute of Biodiversity of Misiones, under the Ministry of Ecology and Renewable Natural Resources of Misiones Province, Argentina.

Previous research has demonstrated the biocontrol effects of *T. koningiopsis* strains (19; 37), and, more recently, the secretion and stability of their cell-wall degrading enzymes (CWDEs) have been optimized (23). All strains were grown in 60 mm Petri dishes containing potato dextrose agar (PDA, 3.9% w/v) with 0.02% w/v chloramphenicol and incubated at  $28 \pm 1$  °C for 7 days.

### Production of enzymatic supernatants by *T. koningiopsis* using *F. oxysporum* cell walls as an inducer

Cell walls of *F. oxysporum* LBM 232 were used as a sole carbon source, at a final concentration of 7

g L<sup>-1</sup>. First, fungal biomass was obtained by culturing *F. oxysporum* in malt extract medium (ME, 2% w/v) at 28 ± 1 °C for 7 days under continuous light. Cell wall extraction was performed according to the method of Cortes *et al.* (1998) (38) with minor modifications. Harvested mycelium was purified by incubation in 0.85% (w/v) NaCl for 2 h, followed by boiling in 2% sodium dodecyl sulfate (SDS) for 5 min to solubilize intracellular components. The resulting material was sequentially washed with chloroform: methanol (1:1, v/v), then with acetone, air-dried, and finally ground using a mortar and pestle.

The nitrogen source was adapted from Mandels medium (39), whose basal composition included KH<sub>2</sub>PO<sub>4</sub> (2 g L<sup>-1</sup>), CaCl<sub>2</sub>·2H<sub>2</sub>O (0.4 g L<sup>-1</sup>), MgSO<sub>4</sub>·4H<sub>2</sub>O (0.3 g L<sup>-1</sup>), FeSO<sub>4</sub>·7H<sub>2</sub>O (0.005 g L<sup>-1</sup>), MnSO<sub>4</sub>·4H<sub>2</sub>O (0.0016 g L<sup>-1</sup>), ZnSO<sub>4</sub>·7H<sub>2</sub>O (0.0014 g L<sup>-1</sup>), and CoCl<sub>2</sub>·6H<sub>2</sub>O (0.02 g L<sup>-1</sup>). The Nitrogen component modified was yeast extract (0.92 g L<sup>-1</sup>).

Assays were conducted under submerged fermentation (SmF) conditions. Erlenmeyer flasks (250 mL capacity) containing 60 mL of culture medium were inoculated with 2.5 mL of a spore suspension (2 × 10<sup>7</sup> spores mL<sup>-1</sup> for both strains). The initial pH of the medium was adjusted to 4.0. Cultures were incubated at 28 ± 1 °C with shaking at 100 rpm for 12 days.

#### **Encapsulation of enzymatic supernatants from *T. koningiopsis* LBM 116 and LBM 219 by ionic gelation**

Enzymatic supernatants were immobilized in sodium alginate via ionic gelation, as described by El-Katatny (2008) (40), with modifications. Under sterile conditions, enzyme supernatants were mixed with a sodium alginate solution at a 1:3 (v/v) ratio. The mixture was extruded dropwise into a sterile CaCl<sub>2</sub> solution using a MAPADA peristaltic pump (Shanghai Mapada Instruments Co., Ltd., China), resulting in instantaneous gelation and capsule formation. Capsules were maintained in CaCl<sub>2</sub> solution for 30 min at room temperature under constant stirring to ensure complete crosslinking. They were then filtered, washed with sterile distilled water, and stored at 5 °C until further use.

#### **Spectrophotometric determination of enzymatic activity**

Protease, β-1,3-glucanase, and chitinase activities were determined spectrophotometrically using modified protocols based on previously described methods (41-46).

For Protease activity, the reaction mixture, consisting of 300 μL of azocasein (0.5%, w/v in Tris-HCl buffer, pH 7.4) and 300 μL of enzyme formulation, was incubated at 37 °C for 50 min. For encapsulated formulations, 300 mg (fresh weight)

of capsules were used per reaction. To terminate the reaction, 600 μL of 10% (w/v) trichloroacetic acid was added, and the mixture was centrifuged at 7000 rpm for 5 min. The absorbance of the supernatant was measured at 340 nm using a Shimadzu UV-Vis 1900 spectrophotometer. Enzyme activity was expressed in units equivalent to the activity of 1 mg of papain (1 unit = 1 mg of papain), based on a standard curve prepared with commercial papain (Sigma-Aldrich) using azocasein as substrate.

β-1,3-glucanase activity was determined using 1% (w/v) laminarin in 0.2 M acetate buffer (pH 5). A reaction mixture containing 250 μL of substrate and 250 μL of enzyme formulation (250 mg for the encapsulated formulations) was incubated at 50 °C for 40 min. The reaction was stopped by adding 500 μL of 3,5-dinitrosalicylic acid (DNS) reagent and boiling for 10 min. After cooling, 4 mL of distilled water was added, and absorbance was measured at 540 nm. One unit (U) of β-1,3-glucanase activity was defined as the amount of enzyme required to release 1 μmol of glucose per minute under the assay conditions.

Chitinase activity was measured using 0.5% (w/v) colloidal chitin prepared in 0.05 M acetate buffer at pH 4.8. A volume of 300 μL of substrate was mixed with 300 μL of enzyme formulation (300 mg for encapsulated formulations) and incubated at 37 °C for 60 min with agitation at 90 rpm. The reaction was stopped by adding 600 μL of DNS reagent (43), followed by boiling for 10 min and centrifugation at 7000 rpm for 5 min. Absorbance was measured at 540 nm. One unit (U) of chitinase activity was defined as the amount of enzyme capable of releasing 1 μmol of N-acetylglucosamine (NAG) per minute under the assay conditions.

#### **Optimization of the encapsulation process**

The encapsulation process was optimized using response surface methodology (RSM) implemented in Statgraphics Centurion XVI (StatPoint, Inc., USA). A Box-Behnken design (BBD) was selected due to its efficiency in evaluating quadratic response surfaces with a reduced number of experimental runs.

Three independent variables were evaluated: sodium alginate concentration (1, 1.5, and 2%), CaCl<sub>2</sub> concentration (1, 1.5, and 2%), and cannula diameter (0.3, 0.5, and 0.7 mm).

To facilitate data interpretation, actual factor levels were converted to standardized units, where 1 represented the highest value and -1 the lowest (Table 1). Seventeen experimental runs were conducted, including five replicates at the center point. The center point, positioned at level 0 for all factors, provided a more reliable estimate of experimental variance across the design space.

**Table 1.** Coded factor levels for RSM-BBD for optimization of the three variables: sodium alginate concentration, CaCl<sub>2</sub> concentration, and cannula diameter.

Factors	Levels		
	-1	0	1
Sodium alginate concentration	1%	1.5%	2%
CaCl <sub>2</sub> concentration	1%	1.5%	2%
Cannula diameter	0.3mm	0.5mm	0.7mm

Immobilization efficiency (EE, %) of each enzyme was used as the response variable and calculated according to the following equation:

$$EE (\%) = \frac{UAE_{encapsulated}}{UAE_{formulation}} \times 100 \quad (1)$$

where UAE<sub>formulation</sub> denotes the enzyme activity units initially present before encapsulation, and UAE<sub>encapsulated</sub> denotes the enzyme activity units retained within the capsules after encapsulation. Experimental data were analyzed using Statgraphics Centurion XVI (StatPoint, Inc., USA). An analysis of variance (ANOVA) within the RSM framework was conducted at a 95% confidence level. Model adequacy was evaluated through lack-of-fit testing and the coefficient of determination (R<sup>2</sup>). Standardized Pareto charts were used to identify significant factors, and three-dimensional response surface plots were generated to visualize interactions among variables. Optimal conditions were determined using multiple-response optimization analysis.

#### Capsule morphological characterization

The morphology of the obtained capsules was evaluated using an optical microscope (Leica DM750, Switzerland). Diameter and circularity were determined for 30 capsules per strain using ImageJ 1.51n software (Wayne Rasband, National Institutes of Health, USA). Measurements were performed at 40× magnification.

The average fresh weight of individual capsules was estimated from ten subsamples per strain. Each subsample was weighed on an analytical balance, and the number of capsules counted. Individual capsule weight was calculated as:

$$Individual\ capsule\ weight\ (g) = \frac{sample\ weight\ (g)}{number\ of\ capsules} \quad (2)$$

#### Enzymatic stability of encapsulated formulations

The stability of encapsulated enzymes was evaluated by incubating capsules at 25 °C in buffer solutions at different pH values. For protease determination, capsules were incubated at pH 6, 7.4, and 8; whereas for β-1,3-glucanases determination, capsules were incubated at pH 4, 5, and 6 (23). The assay was conducted for 10 days, with samples collected every 2 days.

Residual enzymatic activity was expressed as a percentage relative to initial activity (time zero = 100%). Data were analyzed using two-way ANOVA followed by LSD multiple-range tests at the 95% confidence level.

#### Reuseability of immobilized CWDE activities

The reusability of immobilized enzymes was assessed by measuring activity successively using fresh substrate in each cycle. All assays were performed in duplicate. Enzymatic activity was expressed as percentage retention relative to the initial activity. Statistical analysis was conducted using one-way ANOVA at a 95% confidence level.

#### Antifungal activity of encapsulated formulations

Antifungal activity was evaluated under three experimental conditions: (i) cultures inoculated with free enzymatic supernatant, (ii) cultures inoculated with encapsulated enzymatic formulations, and (iii) an untreated control. Assays were conducted in 250 mL Erlenmeyer flasks containing 50 mL of malt extract medium (20 g L<sup>-1</sup>), previously inoculated with 1 × 10<sup>7</sup> spores mL<sup>-1</sup> of the phytopathogen *Fusarium oxysporum* LBM 232.

Free formulations were added at a final volume of 2 mL of crude supernatant per flask, whereas encapsulated treatments received 2 g of freshly prepared capsules. Control flasks contained only the fungal inoculum without enzymatic additions. All treatments were performed in duplicate. Cultures were incubated at 28 ± 1 °C under orbital shaking (100 rpm) for 10 days. At the end of the incubation period, fungal biomass was recovered, dried to constant weight, and expressed as dry weight. Data were analyzed by one-way ANOVA followed by LSD multiple-range tests at a 95% confidence level.

## RESULTS AND DISCUSSION

#### Encapsulation of enzymatic supernatants from *T. koningiopsis* LBM 116 and LBM 219 by ionic gelation

Crude supernatants prior to encapsulation exhibited detectable protease, β-1,3-glucanase, and chitinase activities, confirming the presence of a complete mycolytic enzymatic complex suitable for immobilization. However, after encapsulation, only protease and β-1,3-glucanase activities remained detectable. Notably, chitinase activity was not detected in the encapsulated formulations (Figure 1), indicating that this enzymatic fraction was not retained within the alginate matrix. This may be attributed to the pore size distribution and the intrinsic permeability of pure alginate hydrogels, which can facilitate enzyme diffusion during gelation or subsequent washing steps (47).

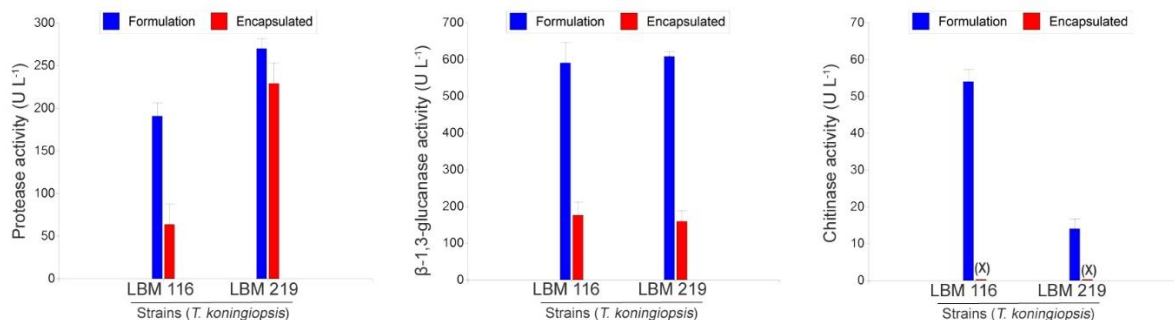


**Figure 1.** Enzymatic activity of crude supernatants (Formulation) and encapsulated formulations (Encapsulated) from *T. koningiopsis* LBM 116 and LBM 219. Protease,  $\beta$ -1,3-glucanase, and chitinase activities are expressed as U L<sup>-1</sup>. Bars represent mean values  $\pm$  standard deviation. The symbol (X) indicates absence of detectable enzymatic activity in the encapsulated formulations.

The detected EE values fall within the expected range for systems based on crude extracts, where enzyme purity, molecular heterogeneity, and medium composition influence retention capacity (40). These baseline activities were used to calculate encapsulation efficiency (EE) within the RSM-BBD framework (Table S1). Protease EE was  $33.3 \pm 12\%$  for *T. koningiopsis* LBM 116 and  $84.8 \pm 8.8\%$  for *T. koningiopsis* LBM 219, whereas for  $\beta$ -1,3-glucanase EE reached  $29.9 \pm 6.0\%$  and  $26.3 \pm 4.7\%$ , respectively.

The overall low EE values, except for proteases from *T. koningiopsis* LBM 219, may be attributed to intrinsic limitations of droplet-based ionic gelation methods. This approach, widely used due to its simplicity and biocompatibility, can exhibit enzyme leaching because of the hydrophilic nature of alginate and the relatively large pore size of its polymer network ( $\sim 200$  nm) (48). In contrast, the incorporation of external coatings or hybrid matrices has been shown to improve retention. Other studies have reported that alginate-chitosan or alginate-pectin composite systems achieved efficiencies of 77–95% for proteases (49–51). These findings suggest that incorporating an external coating or a hybrid matrix could improve EE.

Nevertheless, optimizing the encapsulation process allowed for the identification of physicochemical parameters that significantly affect EE. In particular, the RSM-BBD design enabled the determination of optimal conditions for maximizing proteases and  $\beta$ -1,3-glucanases EE, thereby guiding the development of capsules suitable for the controlled release of biocatalysts.

The coefficients of determination obtained from the ANOVA – RSM analysis for *T. koningiopsis* LBM 116 ( $R^2 = 0.86$  for protease and  $0.90$  for  $\beta$ -1,3-glucanase) together with a non-significant lack-of-fit ( $p > 0.05$  at the 95% confidence level), support the model's suitability for describing the observed data.

For protease activity, the quadratic effect of CaCl<sub>2</sub> was significant ( $p < 0.05$ ), indicating its influence on the curvature of the model (Table S2). The EE results suggest a nonlinear relationship between Ca<sup>2+</sup> concentration and gel crosslinking.

Previous studies have reported formation of amorphous structures at low concentrations, stable spheres at intermediate concentrations, and rigid agglomerates at high concentrations (52–54). These results confirm the critical balance between network density and hydrogel permeability.

For  $\beta$ -1,3-glucanases, statistically significant effects of alginate and the quadratic term of cannula diameter ( $p < 0.05$ ) on EE were detected (Table S3). The Pareto chart shows the negative influence of both variables (Figure 2A).

The RSM model for *T. koningiopsis* LBM 219 yielded  $R^2$  values of  $0.67$  for proteases and  $0.90$  for  $\beta$ -1,3-glucanases. Lack-of-fit was not significant ( $p > 0.05$  at the 95% confidence level), indicating that the selected model was appropriate for describing the observed data.

For proteases, no factor had a statistically significant effect on EE ( $p > 0.05$ ) (Table S4). In contrast, for  $\beta$ -1,3-glucanases, sodium alginate (A) and the quadratic effect of cannula diameter (CC) were significant ( $p < 0.05$ ) (Table S5), both showing negative effects on EE (Figure 2B).

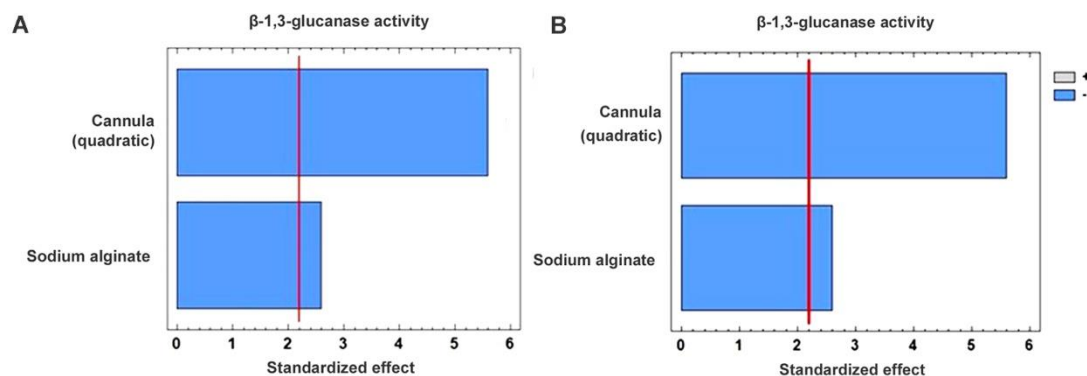


**Figure 2.** Pareto chart showing the factors in decreasing order of significance affecting β-1,3-glucanase activity in **A)** *T. koningiopsis* LBM 116 and **B)** *T. koningiopsis* LBM 219. Bar length is proportional to the standardized effect of each factor on enzymatic efficiency of the encapsulation, with 95% confidence.

Therefore, for β-1,3-glucanases, the effects were comparable between the two strains. This agrees with reports indicating that higher polymer viscosity or larger droplet size can reduce mass transfer and homogeneity, thereby reducing EE (55,53). Conversely, moderate alginate concentrations and small cannula diameters optimize Ca<sup>2+</sup> diffusion and gelation (56). Multiple-response optimization predicted the conditions that maximize desirability within the experimental region, thereby jointly optimizing the

EE of proteases and β-1,3-glucanases in both strains (Figure 3). The optimum conditions, calculated from the model-predicted values, were sodium alginate concentration (1%), CaCl<sub>2</sub> concentration (1%), and cannula diameter (0.5 mm). Based on these results, the RSM model-predicted conditions were validated, and capsules were produced under optimal conditions for subsequent analyses.

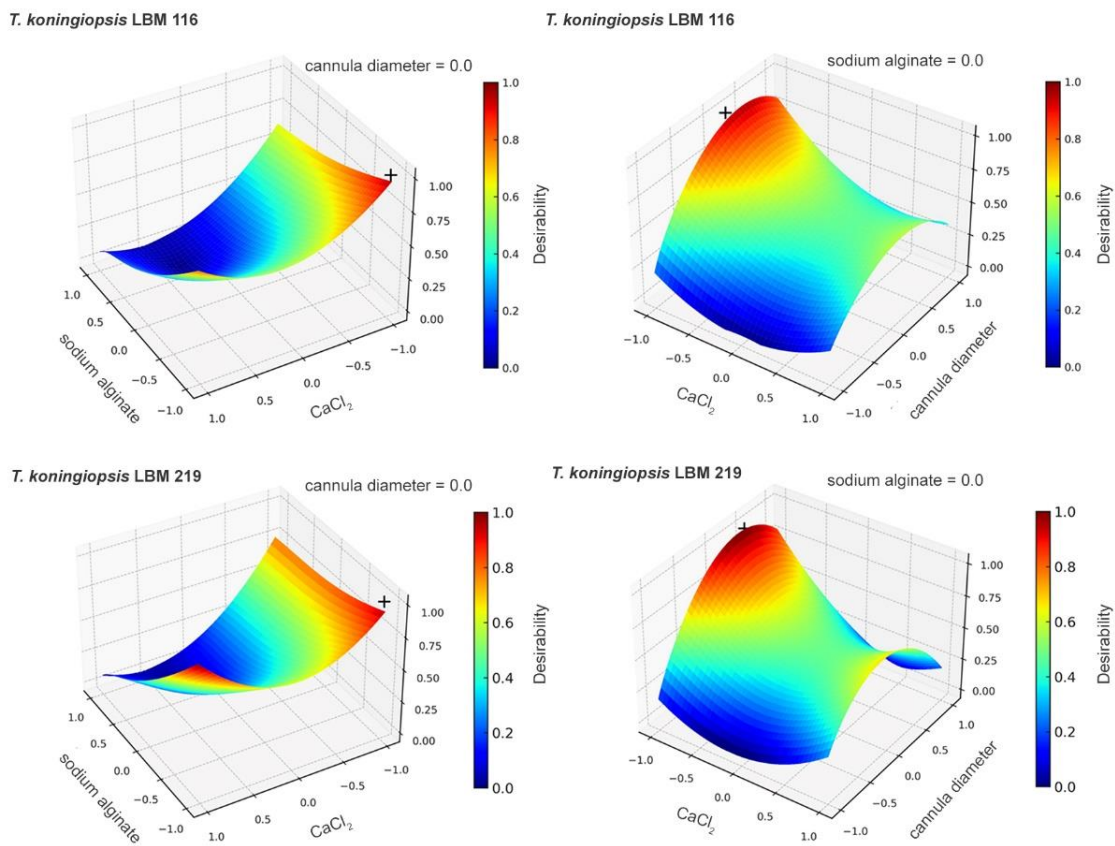


**Figure 3.** Three-dimensional response surface plots of the desirability function showing the predicted optimal conditions (+) within the experimental design space for sodium alginate concentrations, CaCl<sub>2</sub> concentration, and cannula diameter in capsules produced with *T. koningiopsis* LBM 116 and LBM 219.

### Capsule morphological characterization

The capsules obtained from *T. koningiopsis* LBM 116 had an average diameter of  $1318 \pm 109 \mu\text{m}$ , whereas those from *T. koningiopsis* LBM 219 reached  $1355 \pm 98 \mu\text{m}$ . In both strains, average circularity was  $0.92 \pm 0.02$ , reflecting nearly

spherical morphology. Regarding weight, capsules of LBM 219 averaged  $3.22 \pm 0.28 \text{ mg}$ , whereas those of LBM 116 averaged  $2.85 \pm 0.26 \text{ mg}$ . These morphological characteristics are shown in Figure 4.

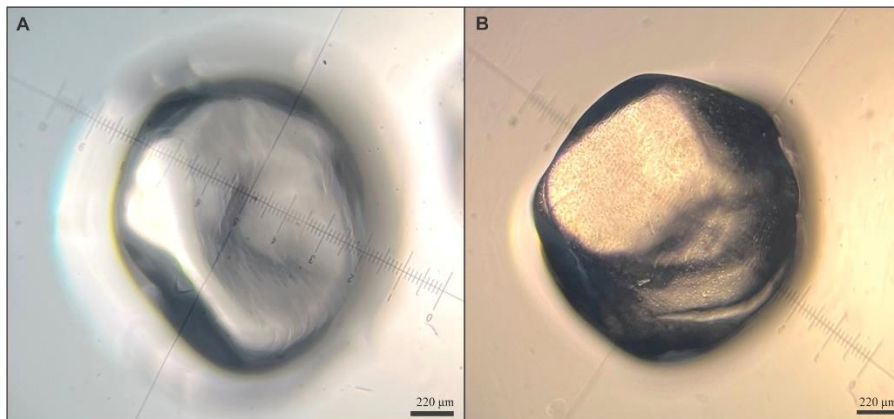


**Figure 4.** Optical micrographs showing capsule morphology of strains *T. koningiopsis* LBM 116 (A) and *T. koningiopsis* LBM 219 (B). Magnification: 4 $\times$ . Scale bars = 220  $\mu\text{m}$ .

These analyses place the beads within the alginate macrocapsule size range ( $>1000 \mu\text{m}$ ) (57). Capsule size was consistent with values reported in the literature for extrusion-based encapsulation systems for immobilization of biological control agents (58).

Furthermore, the spherical and homogeneous morphology of the capsules is a desirable feature, as it directly influences their durability, structural stability during drying or storage, and more predictable biocatalyst release (59).

Additionally, determination of individual capsule weight is a relevant parameter associated with density and dosage standardization, as it enables estimation of the number of functional units per sample and serves as an indirect indicator of the amount of immobilized enzymatic material. This, in turn, improves dosage consistency and reproducibility in antifungal assays (60).

### Enzymatic stability of encapsulated formulations

Evaluation of enzymatic stability in the capsules revealed differential behavior between strains and between protease and  $\beta$ -1,3-glucanase activities. For *T. koningiopsis* LBM 116 capsules, no activity was detected beginning with the first sampling point (day 2). In contrast, *T. koningiopsis* LBM 219 capsules retained activity, with no significant differences across pH levels or over time ( $p > 0.05$ ). These proteases, with an optimum pH close to 7.4 (24), maintain their active conformation in neutral or slightly basic media. In addition, alginate may provide protection under acidic conditions, since at low pH, alginic acid becomes insoluble,

and increased proton ( $\text{H}^+$ ) concentration strengthens ionic bonds between polymer chains, compacting the network and reducing permeability (61). This combination of intrinsic enzyme pH optimum and matrix stability may explain the minimal variation in protease activity across pH values.

For  $\beta$ -1,3-glucanase activity, no significant differences were observed between the two strains ( $p > 0.05$ ), therefore, data were analyzed jointly. Both pH and time had statistically significant effect on enzyme activity ( $p < 0.05$ ). Analysis of pH identified two homogeneous groups: activities at pH 4 and 5 were significantly higher than at pH 6 ( $p < 0.05$ ), suggesting greater stability over time under lower pH values (Figure 5A), consistent with the reported catalytic activity range (24). Within this range, the alginate network remains compact, limiting denaturation and enzyme leakage. However, as pH increases toward more basic values ( $\geq 6$ ), the gel begins to swell and lose structural cohesion, increasing permeability and reducing protection against inactivation (62). The decrease observed at pH 6 may therefore be attributed to the combined effects of the enzyme's intrinsic instability under less favorable pH conditions and weakening of the encapsulating support.

Regarding the time factor, statistical analysis revealed two homogeneous groups ( $p < 0.05$ ): Group 1, including days 0 to 8, and Group 2, consisting of day 10, which showed significantly lower enzymatic activity, indicating loss of stability at the end of the evaluated period (Figure 5B).

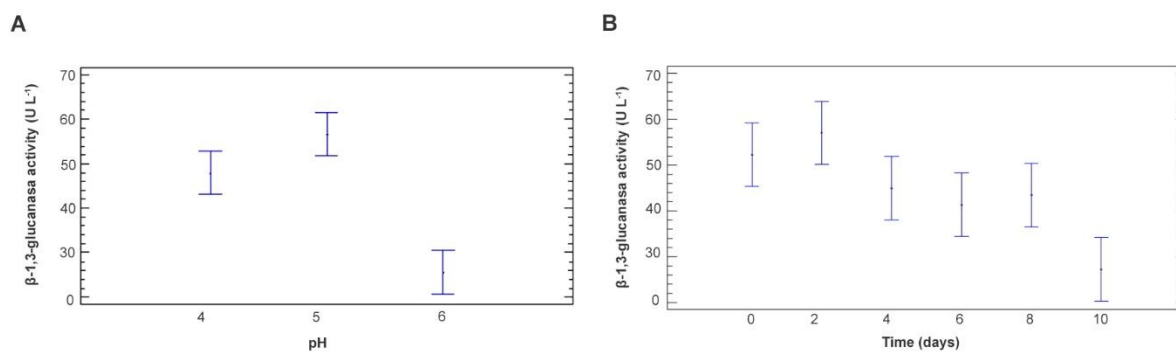


**Figure 5.** Mean plots with 95% confidence intervals (Fisher's LSD) for  $\beta$ -1,3-glucanase enzyme activity (U/mL) as a function of (A) pH and (B) time.

These results demonstrate that the overall system stability depends on the interaction between enzyme pH optimum and the structural response of alginate. Proteases, with a basic optimum and additional protection by gel compaction under acidic conditions, maintained activity over time; whereas the  $\beta$ -1,3-glucanases, which depend on acidic conditions, lost stability as the matrix lost rigidity and provided less effective protection.

#### Reusability of immobilized CWDE activities

During evaluation of the operational reusability of the enzyme capsules, variations in protease and

$\beta$ -1,3-glucanase activity were observed across successive reaction cycles.

Protease activity in *T. koningiopsis* LBM 116 and LBM 219 remained stable throughout the five cycles, maintaining retention percentages close to 100% of the initial activity (Figure 6A and 6B). In both cases, no statistically significant differences over time were observed ( $p > 0.05$ ). This demonstrates high stability and low loss due to diffusion or inactivation, which may be attributed to a favorable interaction between the enzyme and the matrix, associated with larger molecular size or greater surface affinity, thereby reducing leakage and promoting retention (63).

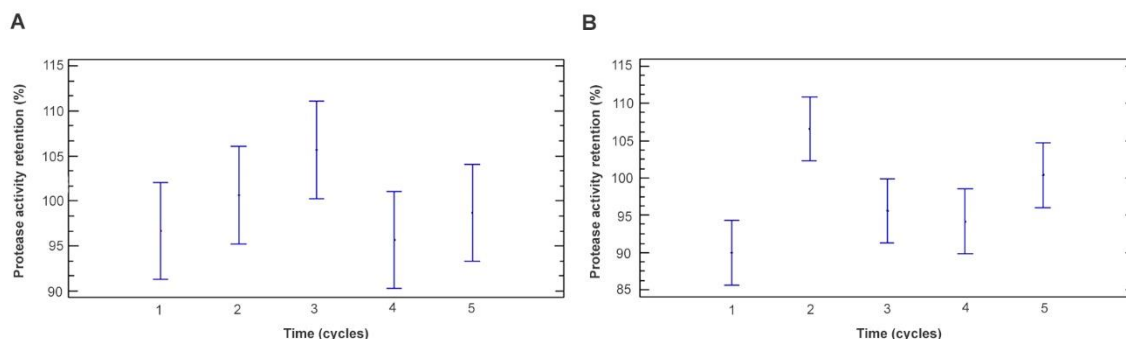


**Figure 6.** Mean plots showing the percentages of retained protease activity in (A) *T. koningiopsis* LBM 116 and (B) *T. koningiopsis* LBM 219. The x-axis represents the five measurement cycles (1–5), whereas the y-axis indicates the percentage of protease activity relative to the initial activity.

$\beta$ -1,3-glucanase activity in capsules from *T. koningiopsis* LBM 116 showed statistically significant differences between cycles ( $p < 0.05$ ), with an abrupt decrease to ~30% in the second cycle and complete loss in subsequent cycles (Figure 7A). In *T. koningiopsis* LBM 219, significant differences were also observed ( $p < 0.05$ ), with activity decreasing to ~85% in the second cycle, followed by complete loss of activity in subsequent cycles (Figure 7B).

This behavior is consistent with previous reports (40; 64). The decrease in activity may be attributed to enzyme leakage caused by matrix porosity. If

the size of the gel pores allow enzyme molecules to pass through, they may diffuse into the medium during successive washes, thereby reducing detectable activity in subsequent cycles. This phenomenon is particularly relevant for small, hydrophilic enzymes, a characteristic frequently associated with  $\beta$ -1,3-glucanases (65; 66). Furthermore, recent studies have shown that repeated exposure to fluctuations in pH, temperature, and ionic concentration may cause progressive inactivation, even in enzymes partially retained in the gel (67).

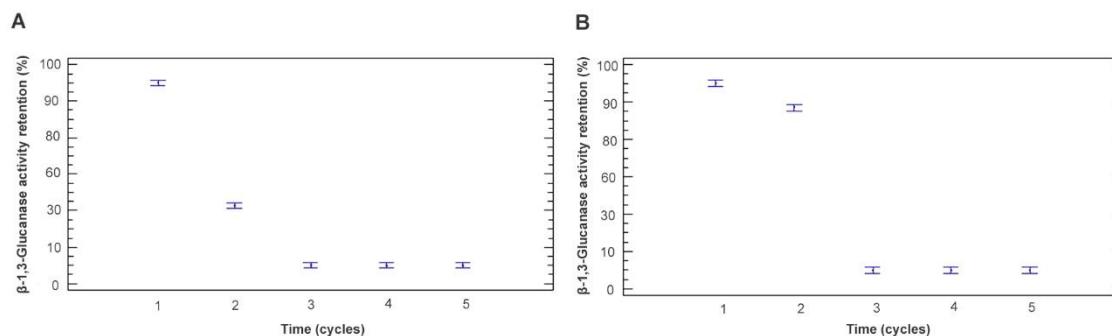


**Figure 7.** Mean plots showing the percentages of retained  $\beta$ -1,3-glucanase activity in *T. koningiopsis* LBM 116 (A) and *T. koningiopsis* LBM 219 (B). The x-axis represents the five measurement cycles (1–5), whereas the y-axis indicates the percentage of protease enzyme activity relative to the initial activity.

### Antifungal activity of encapsulated formulations

One-way ANOVA indicated statistically significant differences in dry weight among treatments and the control ( $p < 0.05$ ). Both free supernatants and

encapsulated formulations from *T. koningiopsis* LBM 116 and LBM 219 significantly reduced the growth of *F. oxysporum* LBM 232 compared with the negative control (Figure 8), confirming the antifungal potential of the enzymatic preparations.

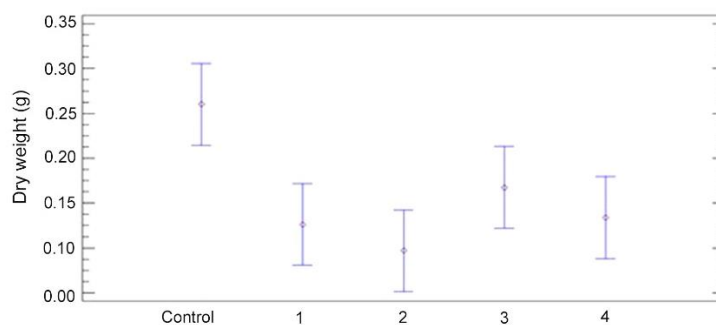


**Figure 8.** Mean dry weight (g) for Control, 1 (LBM 116 capsules), 2 (LBM 219 capsules), 3 (LBM 116 supernatant), and 4 (LBM 219 supernatant). Error bars indicate standard deviation.

These results demonstrate that the mycolytic capsules effectively inhibited pathogen growth, validating the functional preservation of enzymatic activity after immobilization. The observed reduction in fungal biomass suggests a potential inhibitory effect of the enzymatic complex on fungal development.

Alginate, used as the encapsulating matrix, is widely recognized as a biocompatible and biologically inert polymer, commonly employed as a carrier system for bioactive compounds rather than as an active antimicrobial agent (68). Although modified alginate systems or specific derivatives may exhibit antifungal activity, this effect is generally associated with incorporated active compounds or structural modifications rather than with the native polymer itself (69). Therefore, the inhibitory effect observed in this study is likely associated with the cell wall degradation mechanisms described for CWDEs, although further structural analyses are required to confirm this.

Endpoint biomass quantification by dry weight provides an integrative measure of overall

inhibitory effect and is suitable as a preliminary screening approach for enzymatic biocontrol systems (40).

Importantly, although no statistically significant differences were observed between free and encapsulated formulations, the encapsulated systems maintained comparable antifungal efficacy. This finding is particularly relevant from a formulation standpoint, as it indicates that immobilization did not compromise biological activity. Instead, encapsulation provides additional technological advantages, including structural protection, potential stabilization under environmental stress, and controlled release.

### Conclusions

This study demonstrates that ionic gelation using sodium alginate is a feasible strategy for immobilizing enzymatic supernatants from *T. koningiopsis* LBM 116 and LBM 219. The optimization process identified encapsulation conditions that enabled effective retention of protease activity while maintaining antifungal efficacy against *F. oxysporum* LBM 232.

Encapsulation efficiency was enzyme-dependent. Proteases showed high retention and operational stability, whereas  $\beta$ -1,3-glucanases exhibited moderate encapsulation efficiency and progressive loss of activity. Chitinase activity was not retained within the alginate matrix, highlighting structural limitations of pure alginate hydrogels for small or highly diffusible enzymes.

These findings confirm that encapsulation is a promising approach for improving the formulation and field applicability of enzyme-based bioinputs. However, further improvements, such as hybrid matrices or polyelectrolyte coatings, are required to enhance enzyme retention and long-term stability.

### ACKNOWLEDGMENTS

The authors are grateful for the continued support provided by the National University of Misiones, the National Agency for Scientific and Technological Promotion, and the CONICET scholarship program. This work was supported by the National Agency for Scientific and Technological Promotion (16/Q2314-PDTS-FE) and the National University of Misiones (16/Q2851-PI).

### REFERENCES

1. J. Zhu, J. Wang, Y. Ding, B. Liu and W. Xiao, "A systems-level approach for investigating organophosphorus pesticide toxicity," *Ecotoxicology and Environmental Safety*, vol. 149, pp. 26–35, 2018.
2. G. Cacace, "Argentina y los agroquímicos," *Posición. Revista del Instituto de Investigaciones Geográficas*, vol. 8, pp. 1–26, 2022.
3. M. C. Molpeceres, M. L. Zulaica and V. B. Tomaino, "Cuestionamientos al uso de agroquímicos en Argentina y el mundo (2000–2020): Una revisión," *Novum Ambiens*, vol. 1, no. 1, e2340, 2023. doi:10.31910/novamb.v1.n1.2023.2340
4. G. Tripathi and A. Kumar, "Role of bio-inputs in pest management," in *Emerging Trends in Entomology*, Golden Leaf Publishers, p. 183, 2023.
5. V. Valenzuela Ruiz *et al.*, "Regulation, biosynthesis, and extraction of Bacillus-derived lipopeptides and its implications in biological control of phytopathogens," *Stresses*, vol. 4, no. 1, pp. 107–132, 2024.
6. Zhao, G., Zhu, X., Zheng, G., *et al.* (2024). Development of biofertilizers for sustainable agriculture over four decades (1980–2022). *Geogr. Sustain.*, 5(1), 19–28.
7. G. Mustafa *et al.*, "Molecular characterization and mycoparasitic aptitude of indigenous biocontrol agent *Trichoderma harzianum*," *Journal of Animal and Plant Sciences*, vol. 30, no. 6, pp. 1508–1515, 2020.
8. G. A. Bich, M. P. Barengo, N. S. Amerio, F. Duarte, P. D. Zapata and M. L. Castrillo, "Rediscovering fungal biocontrol agents in forestry for sustainable pest management in the north of Argentina," *International Journal of Forestry and Horticulture (IJFH)*, vol. 10, no. 1, pp. 14–19, 2024.
9. K. S. Bhairavi *et al.*, "Biosafety of fungi on nontarget organisms," in *Entomopathogenic Fungi in Insects*, Academic Press, pp. 179–194, 2026.
10. N. Manzar *et al.*, "Trichoderma: Advent of versatile biocontrol agent," *Sustainability*, vol. 14, no. 19, 12786, 2022.
11. Y. Brazhnikova *et al.*, "The antagonistic activity of beneficial fungi and mechanisms underlying their protective effects," *Sustainability*, vol. 17, no. 2, 450, 2025.
12. E. Sepúlveda *et al.*, "Trichoderma in soil ecosystems," in *Soil Microorganisms for Plant Growth Promotion and Soil Health*, Elsevier, pp. 367–386, 2026.
13. N. S. Amerio *et al.*, "Trichoderma en la Argentina: Estado del arte," *Ecología Austral*, vol. 30, no. 1, pp. 113–124, 2020.
14. P. Moya *et al.*, "New isolates of *Trichoderma* spp. as biocontrol agents," *Biological Control*, vol. 141, 104152, 2020.
15. A. Sharma, R. Salwan and V. Sharma, "Extracellular proteins of *Trichoderma* and their role in plant health," *South African Journal of Botany*, vol. 147, pp. 359–369, 2022.
16. P. Guzmán-Guzmán *et al.*, "Trichoderma: A multifunctional agent in plant health," *BMC Microbiology*, vol. 25, 434, 2025.
17. M. E. Laczeski *et al.*, "Isolation and selection of endophytic spore-forming bacteria," *Anais da Academia Brasileira de Ciências*, vol. 92, Suppl. 1, e20181381, 2020.
18. G. Sioli, "Evaluación de la capacidad antagónica...", Tesis de Licenciatura, Universidad Nacional de Misiones, 2014.
19. M. Castrillo *et al.*, "Capacidad biocontroladora de aislamientos nativos de *Trichoderma* sp.," *Chilean Journal of Agricultural & Animal Sciences*, vol. 37, no. 3, pp. 244–256, 2021.
20. Comolli, L. R., Schegg, E., Infuleski, C., Munareto, N., Fassola, H., von Wallis, A., Bulfe, N. M., González, P., Barth, S. R., Gauchat, M. E. and Wyss, F., "Implementing a sustainable integrated agroforestry system for the cultivation of *Ilex paraguariensis*," *Frontiers in Forests and Global Change*, vol. 7, 1424174, 2024. <https://doi.org/10.3389/ffgc.2024.1424174>
21. Quevedo, A. C., Muniz, M. F. B., Sarzi, J. S., Krahn, J. R. T., Savian, L. G., Tabaldi, L. A., Strahl, M. A., Saldanha, M. A., Harakava, R., Poletto, T. and da Silva, J. C. P., "Biocontrol of *Fusarium* spp. root rot in yerba mate (*Ilex paraguariensis*) by native rhizospheric *Trichoderma* spp.," *BioControl*, vol. 69, no. 6, pp. 647–660, 2024. <https://doi.org/10.1007/s10526-024-10271-4>

22. M. P. Barengo, "Caracterización de cepas fúngicas..." Tesis Doctoral, Universidad Nacional de Misiones, 2023.
23. N. S. Amerio et al., "Biotechnological potential of *Trichoderma koningiopsis* LBM116," *Journal of Basic Microbiology*, vol. 65, no. 8, e70062, 2025.
24. N. S. Amerio et al., "Enzymatic strategies for biocontrolling phytopathogenic fungi," *Environmental Microbiology Reports*, vol. 17, no. 3, e70122, 2025. <https://doi.org/10.1111/1758-2229.70122>
25. M. Lorito et al., "Synergistic interaction between fungal cell wall degrading enzymes," *Microbiology*, vol. 140, pp. 623–629, 1994.
26. P. Mishra et al., "Microbial enzymes in biocontrol of phytopathogens," in *Microbial Enzymes: Roles and Applications in Industries*, Springer, pp. 259–285, 2020.
27. S. Somaly, V. Marady, H. Meta and I. Sokra, "Microbial strains for the biological control of gummosis disease: Mechanisms, efficacy, and future prospects," *Journal of Agricultural Science and Technology*, vol. 2, no. 1, pp. 97–108, 2026.
28. M. H. Ly-Chatain, "The factors affecting effectiveness of treatment in phage therapy," *Frontiers in Microbiology*, vol. 5, 51, 2014.
29. L.-N. Yang et al., "Enhanced agricultural sustainability through within-species diversification," *Nature Sustainability*, vol. 2, no. 1, pp. 46–52, 2019.
30. A. P. Felizatti et al., "Encapsulation of *Beauveria bassiana* in biopolymers," *Frontiers in Microbiology*, vol. 12, 704812, 2021.
31. B. Mattiasson, *Immobilized Cells and Organelles*, CRC Press, 2019.
32. M. M. Pour, R. Saberi-Riseh, R. Mohammadinejad and A. Hosseini, "Investigating the formulation of alginate-gelatin encapsulated *Pseudomonas fluorescens* for controlling *Fusarium solani* on potato," *International Journal of Biological Macromolecules*, vol. 133, pp. 603–613, 2019.
33. M. Bhatia, "A review on application of encapsulation in agricultural processes," in *Encapsulation of Active Molecules and Their Delivery System*, Elsevier, pp. 131–140, 2020.
34. J. Baranwal, B. Barse, A. Fais, G. L. Delogu and A. Kumar, "Biopolymer: A sustainable material for food and medical applications," *Polymers*, vol. 14, no. 5, 983, 2022.
35. I. Chibata, *Immobilized Enzymes: Research and Development*, Kodansha, 1978.
36. R. A. Sheldon, "Enzyme immobilization: The quest for optimum performance," *Advanced Synthesis & Catalysis*, vol. 349, no. 8–9, pp. 1289–1307, 2007.
37. A. Pedrozo et al., "ITS identification of the mycoparasitic fungus *Clonostachys rosea* isolated from Misiones soil samples," *Women in Bioinformatics and Data Science Latin America*, 2022.
38. C. Cortes et al., "The expression of genes involved in parasitism by *Trichoderma harzianum* is triggered by a diffusible factor," *Molecular and General Genetics*, vol. 260, pp. 218–225, 1998.
39. M. Mandels and E. T. Reese, "Induction of cellulase in *Trichoderma viride* as influenced by carbon sources and metals," *Journal of Bacteriology*, vol. 73, no. 2, pp. 269–278, 1957.
40. M. El-Katatny, "The activity of  $\beta$ -1,3-glucanase from *Trichoderma harzianum* in native form and after immobilization on calcium alginate," *Archives of Phytopathology and Plant Protection*, vol. 41, no. 3, pp. 175–186, 2008. doi: 10.1080/03235400600679818
41. J. Charney and R. M. Tomarelli, "A colorimetric method for the determination of proteolytic activity," *Journal of Biological Chemistry*, vol. 171, no. 2, pp. 501–505, 1947.
42. M. P. Barengo et al., "Standardization of the azocasein quantitative method to determine proteolytic activity in fungal supernatants," *Bioteconología Aplicada*, vol. 37, no. 2, pp. 2201–2206, 2020.
43. M. M. Kole, I. Draper and D. F. Gerson, "Protease production by *Bacillus subtilis* in oxygen-controlled fermentations," *Applied Microbiology and Biotechnology*, vol. 28, no. 4–5, pp. 404–408, 1988.
44. E. I. Masih and B. Paul, "Secretion of  $\beta$ -1,3-glucanases by the yeast *Pichia membranifaciens*," *Current Microbiology*, vol. 44, no. 6, pp. 391–395, 2002.
45. K.-J. Kim, Y.-J. Yang and J.-G. Kim, "Purification and characterization of chitinase from *Streptomyces* sp. M-20," *BMB Reports*, vol. 36, no. 2, pp. 185–189, 2003.
46. G. L. Miller, "Use of dinitrosalicylic acid reagent for determination of reducing sugar," *Analytical Chemistry*, vol. 31, no. 3, pp. 426–428, 1959.
47. L. S. Ferraraccio et al., "Enzymes Encapsulated within Alginate Hydrogels," *Analytical Chemistry*, vol. 94, no. 46, pp. 16122–16131, 2022. doi: 10.1021/acs.analchem.2c03389.
48. Y. Weng et al., "Alginate-based materials for enzyme encapsulation," *Advances in Colloid and Interface Science*, vol. 318, 102957, 2023. doi: 10.1016/j.cis.2023.102957
49. K. F. Mahmoud et al., "Micro- and nano-encapsulated fungal pectinase," *Food Science and Technology International*, vol. 24, no. 4, pp. 330–340, 2018. doi: 10.1177/1082013217753898
50. F. Bialas et al., "Biomimetic and biopolymer-based enzyme encapsulation," *Enzyme and Microbial Technology*, vol. 150, 109864, 2021. doi:10.1016/j.enzmictec.2021.109864

51. A. da S. Pereira et al., "Polymers as encapsulating agents," *Polymers*, vol. 13, no. 23, 4061, 2021. doi: 10.3390/polym13234061

52. J. Walczak, J. Marchewka and J. Laska, "Hydrogels based on ionically and covalently crosslinked alginates," *Engineering of Biomaterials*, vol. 132, pp. 17–23, 2015.

53. Q. Qi et al., "Preparation of *Trichoderma asperellum* microcapsules and biocontrol of cucumber powdery mildew," *Microbiology Spectrum*, vol. 11, no. 3, 2023. doi: 10.1128/spectrum.05084-22

54. E. Taqieddin and M. Amiji, "Enzyme immobilization in alginate–chitosan microcapsules," *Biomaterials*, vol. 25, no. 10, pp. 1937–1945, 2004.

55. K. Won et al., "Optimization of lipase entrapment in Ca-alginate gel beads," *Process Biochemistry*, vol. 40, no. 6, pp. 2149–2154, 2005.

56. L. Tavernini et al., "Encapsulation of glycosidases in alginate beads," *Catalysts*, vol. 11, no. 7, 866, 2021. doi:10.3390/catal11070866

57. M. Y. Wang et al., "The cell-loaded alginate microspheres in cell culture and disease treatment," *Smart Materials in Medicine*, vol. 6, pp. 387 – 405, 2025.

58. Y. Martinez et al., "Biotechnological development of *Trichoderma*-based formulations," *Applied Microbiology and Biotechnology*, vol. 107, no. 18, pp. 5595–5612, 2023. doi:10.1007/s00253-023-12687-x

59. L. D. Arias-Chavarría et al., "Evaluation of the viability of microencapsulated *Trichoderma longibrachiatum* conidia," *Frontiers in Chemistry*, vol. 12, 2025. doi: 10.3389/fchem.2024.1473217

60. Izquierdo Herrera, P., "Microencapsulación de *Trichoderma viride* contra los principales hongos fitopatógenos de la rizósfera del jitomate (*Solanum lycopersicum*)," Tesis Doctoral, Universidad Autónoma Chapingo, 2017.

61. M. Cruz-Barrera et al., "Hydrogel capsules as delivery system for *Trichoderma*," *World Journal of Microbiology and Biotechnology*, vol. 40, no. 4, 2024. <https://doi.org/10.1007/s11274-024-03897-0>

62. N. Almassri et al., "Evaluation of alginate beads for microencapsulation of enzymes," *Preprints*, 2025. doi: 10.20944/preprints202502.0158.v1.

63. M. Prokopijević, "Natural polymers: suitable carriers for enzyme immobilization," *Biologia Serbica*, vol. 43, no. 1, pp. 43–49, 2021.

64. P. Priyanka et al., "Solvent stable microbial lipases," *Biotechnology Letters*, vol. 41, no. 2, pp. 203–220, 2019.

65. S. Geethanjali and A. Subash, "Optimization and immobilization of purified *Labeo rohita* visceral protease," *Enzyme Research*, 2013. DOI: 10.1155/2013/874050

66. T. Jesionowski, J. Zdarta and B. Krajewska, "Enzyme immobilization by adsorption: A review," *Adsorption*, vol. 20, no. 5–6, pp. 801–821, 2014.

67. H. M. El-Shora et al., "Immobilization of purified pectinase on chitosan and alginate beads," *Microbial Cell Factories*, vol. 24, no. 1, 2025. doi: 10.1186/s12934-024-02603-x

68. Spadari, C. de C., Lopes, L. B. and Ishida, K., "Potential use of alginate-based carriers as antifungal delivery system," *Frontiers in Microbiology*, vol. 8, 97, 2017. <https://doi.org/10.3389/fmicb.2017.00097>

69. Tøndervik, A., Sletta, H., Klinkenberg, G., Emanuel, C., Powell, L. C., Pritchard, M. F., Khan, S., Craine, K. M., Onsøyen, E., Rye, P. D., Wright, C., Thomas, D. W. and Hill, K. E., "Alginate oligosaccharides inhibit fungal cell growth and potentiate the activity of antifungals against *Candida* and *Aspergillus* spp.," *PLOS ONE*, vol. 9, no. 11, e112518, 2014. <https://doi.org/10.1371/journal.pone.0112518>

**Supplementary Information**

**Table S1.** Free and immobilized enzyme activity and immobilization efficiency (%) for proteases and  $\beta$ -1,3-glucanases in the POS7 and TrichoH strains, evaluated in 17 Box-Behnken design assays.

LBM 116		Free protease activity (U L <sup>-1</sup> )	190.9	Free $\beta$ -1.3-glucanase activity (U L <sup>-1</sup> )	591.12
LBM 219		Immobilized protease activity (U L <sup>-1</sup> )	270	Immobilized $\beta$ -1.3-glucanase activity (U L <sup>-1</sup> )	608.4
Strain	Assay	protease activity (U L <sup>-1</sup> )	EE (%) <sup>protease</sup>	glucanase activity (U L <sup>-1</sup> )	EE (%) <sup><math>\beta</math>-1.3-glucanase</sup>
LBM 116	1	112.727	59.048	211.018	35.698
	2	86.364	45.238	214.174	36.232
	3	90.000	47.143	214.174	36.232
	4	53.636	28.095	183.513	31.045
	5	50.000	26.190	150.598	25.477
	6	45.455	23.810	100.098	16.934
	7	80.000	41.905	187.121	31.655
	8	50.000	26.190	122.643	20.748
	9	60.000	31.429	134.817	22.807

	10	37.273	19.524	145.638	24.638
	11	105.455	55.238	189.375	32.037
	12	59.091	30.952	157.813	26.697
	13	31.818	16.667	198.393	33.562
	14	39.091	20.476	202.902	34.325
	15	60.000	31.429	217.781	36.842
	16	49.091	25.714	197.491	33.410
	17	71.818	37.619	172.241	29.138
<b>LBM 219</b>	1	270.909	100	180.808	29.718
	2	267.273	98.990	214.174	35.203
	3	261.818	96.970	174.045	28.607
	4	214.545	79.461	103.254	16.971
	5	220.000	81.481	101.451	16.675
	6	212.727	78.788	137.522	22.604
	7	227.273	84.175	138.875	22.826
	8	210.000	77.778	169.536	27.866
	9	213.636	79.125	157.362	25.865
	10	232.727	86.195	160.518	26.383
	11	250.000	92.593	142.933	23.493
	12	217.273	80.471	155.558	25.568
	13	198.182	73.401	179.906	29.570
	14	190.909	70.707	167.281	27.495
	15	243.636	90.236	187.571	30.830
	16	246.364	91.246	179.004	29.422
	17	219.091	81.145	166.379	27.347

**Table S2.** RSM ANOVA for protease activity in *T. koningiopsis* LBM116. with a 95% confidence level.

Source	Sum of Squares	DF	Mean Square	F-Ratio	P-Value
A: Sodium Alginate	324.526	1	324.526	4.61	0.0982
B: CaCl <sub>2</sub>	532.016	1	532.016	7.56	0.0514
C: Cannula diameter	355.538	1	355.538	5.05	0.0879
AA	198.666	1	198.666	2.82	0.1682
AB	6.85916	1	6.85916	0.10	0.7705
AC	44.4556	1	44.4556	0.63	0.4712
BB	569.601	1	569.601	8.10	0.0466
BC	38.3223	1	38.3223	0.54	0.5015
CC	58.4629	1	58.4629	0.83	0.4136
lack-of-fit	70.3521	3	23.4507	0.33	0.8033
Pure error	281.451	4	70.3627		
Total (corr.)	2490.27	16			

**Table S3.** RSM ANOVA for β-1.3-glucanase activity in *T. koningiopsis* LBM 116. with a 95% confidence level.

Source	Sum of Squares	DF	Mean Square	F-Ratio	P-Value
A: Sodium Alginate	72.6193	1	72.6193	9.41	0.0374
B: CaCl <sub>2</sub>	8.32728	1	8.32728	1.08	0.3576
C: Cannula diameter	56.6101	1	56.6101	7.33	0.0536
AA	2.35234	1	2.35234	0.30	0.6103
AB	8.18246	1	8.18246	1.06	0.3614
AC	1.39712	1	1.39712	0.18	0.6924
BB	18.4589	1	18.4589	2.39	0.1969
BC	12.8558	1	12.8558	1.67	0.2664
CC	341.39	1	341.39	44.22	0.0027
lack-of-fit	27.7428	3	9.24759	1.20	0.4172

Pure error	30.8786	4	7.71966
Total (corr.)	576.504	16	

**Table S4.** RSM ANOVA for protease activity in *T. koningiopsis* LBM 219. with a 95% confidence level

Source	Sum of Squares	DF	Mean Square	F-Ratio	P-Value
A: Sodium Alginate	97.6224	1	97.6224	1.10	0.3525
B: CaCl <sub>2</sub>	97.6363	1	97.6363	1.11	0.3525
C: Cannula diameter	11.1109	1	11.1109	0.13	0.7408
AA	76.986	1	76.986	0.87	0.4034
AB	65.3026	1	65.3026	0.74	0.4384
AC	3.4299	1	3.4299	0.04	0.8534
BB	291.218	1	291.218	3.30	0.1436
BC	92.0832	1	92.0832	1.04	0.3650
CC	108.124	1	108.124	1.22	0.3307
lack-of-fit	56.3133	3	18.7711	0.21	0.8831
Pure error	353.394	4	88.3485		
Total (corr.)	1242.73	16			

**Table S5.** RSM ANOVA for  $\beta$ -1.3-glucanase activity in *T. koningiopsis* LBM 219. with a 95% confidence level.

Source	Sum of Squares	DF	Mean Square	F-Ratio	P-Value
A: Sodium Alginate	72.6193	1	72.6193	9.41	0.0374
B: CaCl <sub>2</sub>	8.32728	1	8.32728	1.08	0.3576
C: Cannula diameter	56.6101	1	56.6101	7.33	0.0536
AA	2.35234	1	2.35234	0.30	0.6103
AB	8.18246	1	8.18246	1.06	0.3614
AC	1.39712	1	1.39712	0.18	0.6924
BB	18.4589	1	18.4589	2.39	0.1969
BC	12.8558	1	12.8558	1.67	0.2664
CC	341.39	1	341.39	44.22	0.0027
lack-of-fit	27.7428	3	9.24759	1.20	0.4172
Pure error	30.8786	4	7.71966		
Total (corr.)	576.504	16			